

# SLOTTED THIN SHELL DEPLOYABLE REFLECTORS

Lin Tze Tan\*

*Department of Civil & Environmental Engineering,  
University College London, Gower Street, London WC1E 6BT, UK,  
l.tan@ucl.ac.uk*

## ABSTRACT

The need for compactly packaged, lightweight and yet high accuracy reflector antennas has led to a novel design for a thin slotted shell reflector antenna. This paper details a new design and experiments for a compactly folded reflector which uses its stored elastic strain energy from the folding process to power deployment – without any expensive motors or hinges. Key to the design are different sets of slits/slots which relieve the membrane stresses in the shell and hence allow the synclastic reflector to be folded compactly and elastically in a nearly inextensional manner – making it practical for smaller satellite missions. A defining feature of the reflector is an integral stiffening rim which is essential in maintaining the deployed shape accuracy and overall structural integrity, this stiffening rim acts to double the deployed stiffness of the reflector. Through detailed finite element analyses we also show that the deployed stiffness is only 3.5% lower while the initial stiffness is 50% better and the stowage ratio is at least 35% better than the current highest stiffness single-piece thin shell reflector design.

## 1. INTRODUCTION

The recent availability of high-modulus, ultra-thin composite materials has led to the realization of novel ultra thin shell deployable reflector structures[3, 7, 8, 13] which do not require further backing support structures. The deployment process of the majority of these thin shell deployable structures is powered by the elastic strain energy which is stored up in the structure from the folding process. This is a simple yet highly elegant technique of powering deployment as no motors or drives are required, hence significantly reducing the chances of anomalies in orbit. In order to fold a structure elastically, the structure must first be highly flexible, however this conflicts with the high shape accuracy requirements for most aerospace structures and is a severe limitation on the applicability of these structures. A method of stiffening these inherently 'floppy' structures has been previously presented [11, 10] and involves an integral stiffening rim which stiffens the structure in its deployed configuration but is designed

to form localized elastic buckles during the folding process hence rendering the entire structure still flexible enough to be folded elastically.

This paper describes a new design of a thin shell reflector which combines this integral stiffening rim with the inclusion of several sets of incisions or slots in the synclastic surface of the dish. This results in an elastically folded ultra light weight design with an improved packaging efficiency, a high deployed stiffness and good shape accuracy.

It will be shown that the initial stiffness of this deployable slotted shell reflector antenna (DeSSRA) is at least 50% higher than the current best performing thin shell reflector antenna – Tan & Pellegrino's Stiffened Spring Back Reflector[8, 2, 9], while its packaging ratio is at least 35% more efficient.

## 2. ULTRA THIN SHELL REFLECTORS

Reflector antenna design is driven by weight, surface accuracy and packaging requirements; membrane reflectors are the most light-weight and compactly packaged but lack the required accuracy, whereas solid surface reflectors have high accuracies but have large masses and large stowage volumes due to the support structure. The advent of high stiffness ultra thin carbon fiber reinforced plastic materials have led to a new class of reflector design which is theoretically able to integrate the high surface accuracy of solid surface designs with the low masses of membrane designs. These ultra thin shell ( $t < 3\text{mm}$ ) reflector designs can be further divided into two main categories: a) segmented and b) single piece designs.

### 2.1. Segmented thin shell reflectors

Notable examples of this type of reflector are Greschik's pop-up reflectors[3] and Tibbalds *et al* thin shell slit reflector[13], Figure 1. These reflectors are characterized by their segmented or 'petal' architecture which lead to very efficient stowage ratio but require deployment devices in the form of zipping devices[13] to reconnect the petals.

---

\*Lecturer in Structural Mechanics

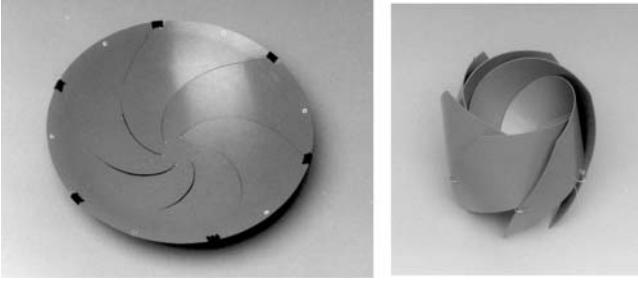


FIG. 1: Small scale model of segmented or petalized reflector in deployed and packaged configuration from Ref.[13]

## 2.2. Single piece thin shell reflectors

Examples of these include the Boeing/Hughes Spring Back Reflector (SBR) [5], Composite Optics furlable reflector [6] and Tan & Pellegrino's Stiffened Spring Back Reflector(SSBR) [12]. The common feature of these designs is the packaging of the reflector as a single piece which is in most cases folded into a 'taco shell' configuration, Figure 2. There is hence no need for reconnection devices and hence only a pyrotechnic bolt is required to release the stored strain energy and deploy the reflector. So far the only method of folding these structures has been to roll it up; hence while one diameter can be halved the other is increased resulting in a long 'cigar' shape or an extreme aspect ratio, which for smaller satellite missions is not always practical.

Since the majority of these thin shell reflectors are flexible enough to fold elastically and hence utilize the stored strain energy to power deployment, they are highly susceptible to manufacturing distortions which can be of the order of  $D/1000$  in an unstiffened thin parabolic dish ( $D=4.6$  m). This is a severe limitation on the operating frequency range and applicability of the reflector.

The Stiffened Spring Back Reflector overcomes this problem by virtue of an integral stiffening rim. This collapsible stiffening rim significantly increases the overall stiffness of the dish in the deployed configuration and yet when it is being packaged, localized buckles form in the rim and hence reduce the overall stiffness of the structure allowing it to still be folded elastically. A recent study commissioned by the European Space Agency [2] to compare leading state of the art reflector designs found the SSBR to be the design with the lowest mass and highest deployed frequency but with a very low packaging efficiency.

## 3. DEPLOYABLE SLOTTED SHELL REFLECTOR ANTENNA

Previous studies have shown that the integral stiffening rim of the SSBR can increase the deployed stiffness by a factor of 31, and the fundamental frequency by a factor of 4 for only a 16% mass increase [11, 10]. Hence



FIG. 2: Small scale model of the Stiffened Spring Back Reflector in deployed and packaged configuration

the new design for a deployable slotted shell reflector antenna (DeSSRA) will be a single piece thin shell reflector which utilizes this stiffening rim to maintain high deployed stiffness, yet has an increased packaging efficiency.

### 3.1. Design Philosophy

During the packaging process, the overall stiffness of the shell is first reduced by forming localized buckles in the stiffener. In the SSBR design a minimum of 4 rim slits (subtending an angle  $\alpha$ ) are required to buckle the stiffener and hence allow the structure to fold into the taco shell shape.

In order to achieve a higher and more uniform packaging ratio the new design is packaged by pulling four opposite points (instead of two for the SSBR design) along diameters  $d_1$  and  $d_2$  (Figure 4) towards the center of the reflector as in Figure 5. Using the SSBR as a starting point, the resultant stresses due to this 4 point folding system are illustrated in Figure 3(a). This initial analysis demonstrates that the largest stresses occur at 1) the rim, in the sections between the existing slits of the SSBR design and 2) at a radius of about 95 mm from the center of the dish.

Firstly the stress concentrations at the rim are counteracted by inserting another set of rim slits subtending an angle  $\beta$ . These are spaced  $\pi/4$  radians from the original SSBR slits (Figure 4). An additional advantage of these extra rim slits is that they act to further reduce the resistance of the stiffener by inducing elastic buckling in 4 extra regions of the stiffener, significantly reducing the overall stiffness of the reflector.

Once the rim stiffness has been reduced, the four-way folding of the doubly curved dish surface itself can then in theory be achieved with another 8 dish slits or 'slots' placed about  $R/2$  in from the rim. However Figure 3 shows that a less complex pattern of 2 pairs of slots i.e. 4 slots (Figure 4) is sufficient. In order to allow for the maximum bending radii and hence minimizing the packaged stresses in all four quadrants, the 4 slots span  $\pi/2$  radians each and hence need to be staggered along the radius, with one pair at a radius of  $r_1 = 110$  mm and the other 15 mm further in towards

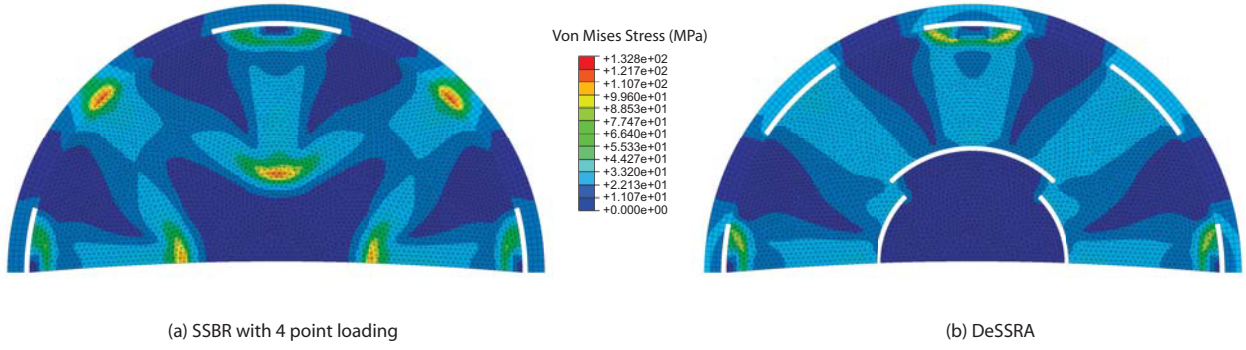


FIG. 3: Stress relieving effect of slots

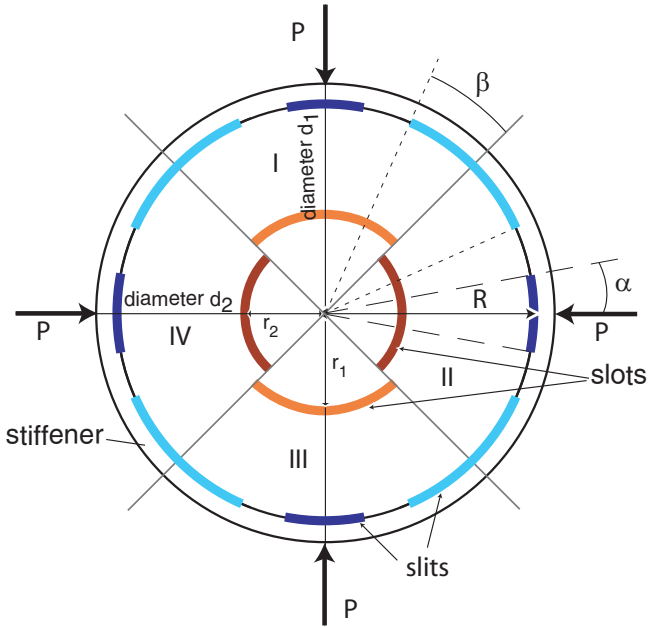


FIG. 4: Geometry of reflector

the center at a radius of  $r_2 = 95$  mm. This results in the packaged configuration shown in Figure 5 with four inward and four outward facing folds. The resulting stress distribution of this new design is shown in Figure 3(b) and demonstrates the effectiveness of the slits/slots in relieving the membrane stresses in the doubly curved shell, hence enabling the synclastic surface to fold in a nearly inextensional manner.

#### 4. COMPUTATIONAL DETAILS

The particular structure that has been analyzed has a uniform thickness of  $t = 1$  mm and forms an axisymmetric paraboloid of equation  $z = \frac{x^2+y^2}{4F}$  where  $F$  is the focal length. The focus to diameter ratio is  $\frac{F}{D} = 0.28$ , the diameter of the aperture is  $D = 450$  mm and hence, the height of the rim above the apex is  $h_0 = 95.6$  mm. From previous work [10] an optimum value of the stiffener width was found to be 20 mm.

The material properties were based on Polyethylene Terephthalate Glycol Modified, PETG, a thermoplastic material from which several experimental dishes were manufactured. The properties of PETG are  $E = 2$  GPa,  $\rho = 1270$  kg/m<sup>3</sup> and  $\nu = 0.3$ .

To keep computational times low, half the dish was analyzed, using the appropriate boundary conditions. Rigid body motions were constrained by fixing the hub of the reflector at a radius of  $D/10$ .

Consistent convergence was achieved with a fine mesh of general purpose, linear 3-noded triangular shell elements (S3R) – average density of 1000 elements per quarter mesh – together with the default ABAQUS iteration control parameters. The stiffening rim was modelled with quadrilateral S4R elements which form surface parallel to the plane of the rim. While the slits and slots were modelled as finite width cut-outs from the reflector surface, for the current case  $\alpha = \beta$  hence all rim slits are equal in length.

All simulations were performed with the ABAQUS finite element package [4] and consisted of two main steps, the first being an eigenvalue extraction to establish the fundamental frequency of the deployed configuration. This fundamental natural frequency is used as a measure of the reflector’s stiffness in the deployed configuration. The second step which models the packaging process is a geometrically non linear static analysis under displacement control, imposing a displacement  $\approx R/2$ . For a more realistic simulation a rectangular region was loaded rather than a single point. The initial resistance to bending  $k$ , peak snapping force  $F_{peak}$ , the final packaged force  $F_{final}$  and the peak stress  $\sigma_{max}$  can be extracted from this latter step. The initial resistance to bending is used as a further indication of the reflector’s deployed stiffness while the peak snapping force is taken as the force before which any snapping or buckling phenomena occur.

In order to provide benchmarks for the DeSSRA design, three other designs were considered;

- DeSSRA – slotted shell design with stiffener, 8 rim slits and 4 dish slots.
- SSBR – reflector with 4 rim slits which are equal

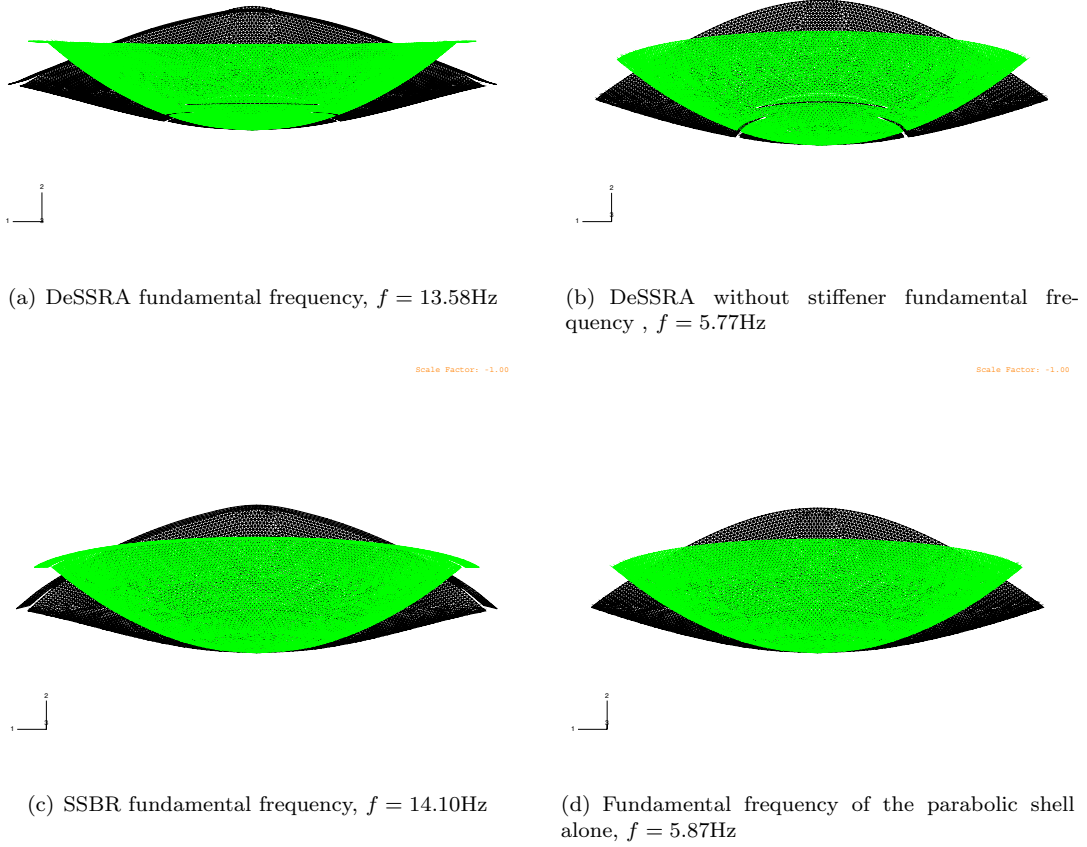


FIG. 6: Natural frequencies of reflector designs

in length to the shortest set of DeSSRA's rim slits and no dish slots. This configuration forms an upper bound value for the deployed stiffness, as there are no dish slots and only one set of rim slits. It is also currently the highest stiffness single-piece thin shell reflector design and hence an upper bound on the deployed frequency.

- DeSSRA with no stiffener – a dish without a stiffener but with the same dish slots as DeSSRA, hence demonstrates the effect of the stiffener.
- SBR – basically a plain parabolic dish with no dish slots or stiffener hence no rim slits. This forms a lower bound on the packaging forces and maximum packaged stresses.

It needs to be noted that both the SBR and SSBR are loaded at *two* diametrically opposite points whereas the slotted shell designs (DeSSRA and DeSSRA without stiffener) are loaded at *four* points.

#### 4.1. Finite Element Model Verification

A simple verification of the finite element model is to analytically estimate the fundamental natural fre-

quency of the parabolic dish. This can be obtained by approximating the dish with a spherical cap of uniform thickness. Using the derivation given in Ref [11], the spherical equivalent of the reflector has an equivalent spherical radius of 302 mm and a subtended angle of  $\phi = 48.12^\circ$ .

An analytical expression for the fundamental natural frequency of vibration of a deep ( $h_0 \geq D/8$ ), open spherical shell was originally obtained by Rayleigh and is available in Blevins[1]

$$(1) \quad f = \frac{\lambda}{2\pi r_m} \sqrt{\frac{E}{\rho}}$$

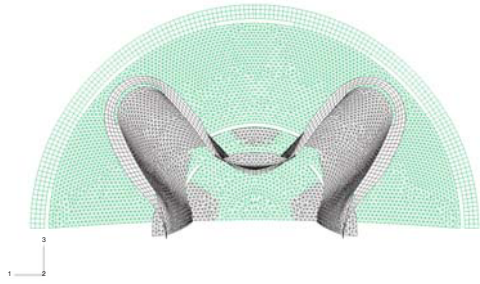
where

$$(2) \quad \lambda = \sqrt{\frac{12}{3(1+\nu)} \left(\frac{t}{r_m}\right)^2 \frac{g_1}{g_2}}$$

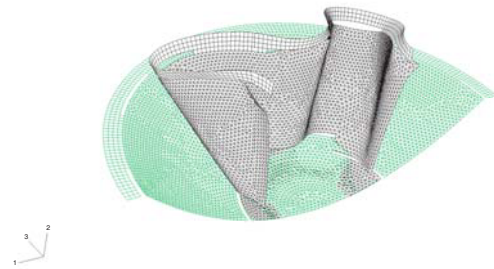
where

$$g_1 = \frac{1}{8} \left[ \left(\tan \frac{\phi}{2}\right)^2 + \left(\tan \frac{\phi}{2}\right)^4 + \frac{\left(\tan \frac{\phi}{2}\right)^6}{3} \right]$$

$$g_2 = \int_0^\phi [(2 + \cos \phi)^2 + 2(\sin \phi)^2] \left(\tan \frac{\phi}{2}\right)^4 \sin \phi \, d\phi$$



(a) Plan view of deployed and folded DeSSRA



(b) Isometric view of deployed and folded DeSSRA

FIG. 5: DeSSRA configuration

Hence for a spherical cap with a 1 mm thickness, the radius to mid surface,  $r_m = 302.5$  mm,  $g_1 = 0.03$ ,  $g_2 = 0.034$ ,  $\lambda = 9.498 \times 10^{-3}$  and hence the fundamental frequency,  $f = 6.27$  Hz. The finite element simulation of the paraboloidal plain SBR shell has a fundamental bending frequency of 5.90 Hz leading to a difference of 5.9% which is due to the fact that the analytical estimate is for the equivalent spherical cap and not the actual paraboloid.

## 5. EXPERIMENTS

Packaging experiments were carried out on small scale Vivak (PETG) dishes made by vacuum forming on parabolic moulds with conical edges. The exact dimensions of these dishes are  $D = 350$  mm,  $F/D = 0.4$  and stiffener width of 25 mm. Note these had to be have different dimensions due to limitations in the vacuum former. The models were mounted vertically on an INSTRON machine at four loading points which were linked with cables in order to impose an equal force rate at each loading point(see Fig. 7). However in order to isolate the forces acting along the different diameters, only one loading point was connected to the INSTRON load cell. The loading points were connected through ball and socket fittings to allow for free rotation of these points.



FIG. 7: Experimental Setup

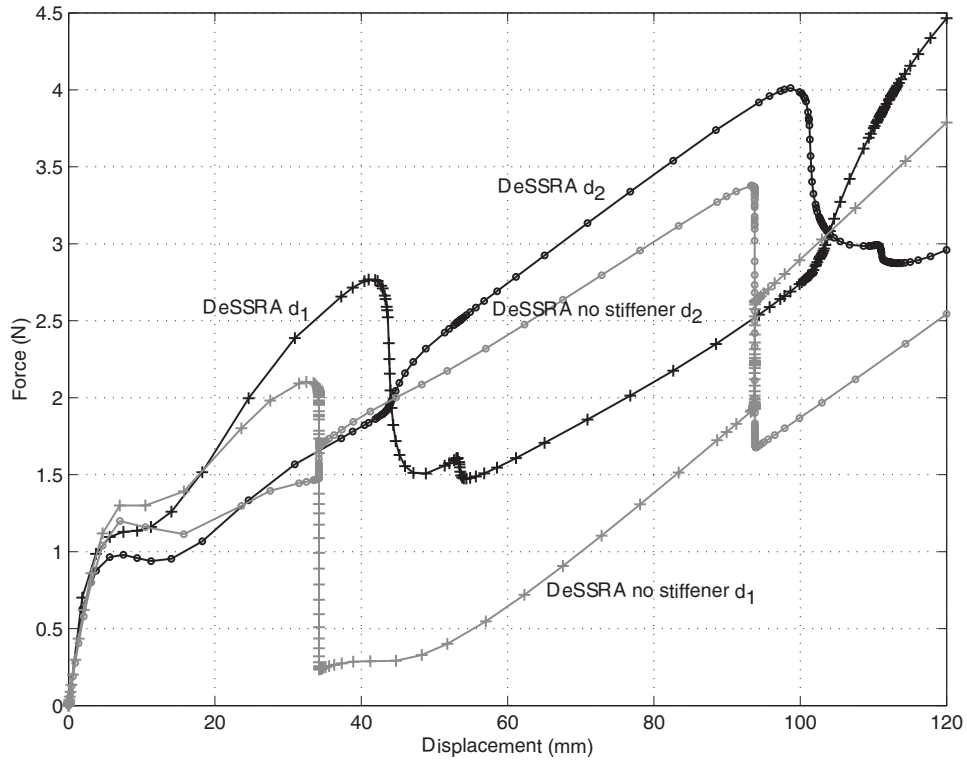
## 6. RESULTS & DISCUSSION

The fundamental natural frequencies and mode shapes of these four designs which manifest themselves as bending modes are shown in Figure 6. The corresponding frequencies are also listed in Table 1, the results demonstrate the significant effect the stiffener has on the deployed stiffness of the reflector –the removal of the stiffener which accounts for 12% added mass reduces the deployed frequency by 57% .

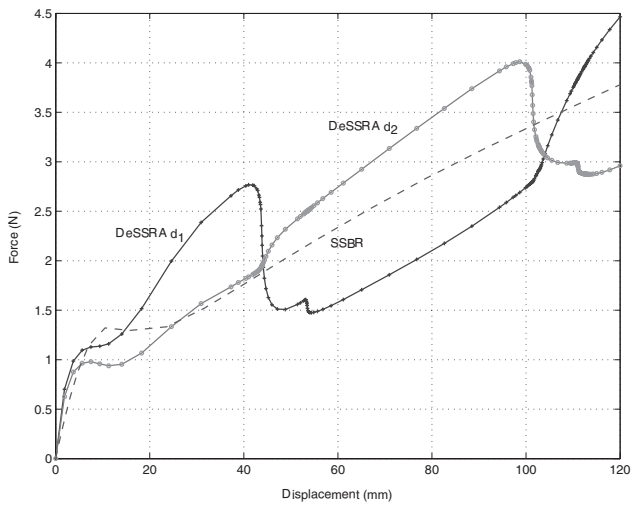
The 1.7% drop in frequency between the DeSSRA without stiffener configuration and the SBR leads to the conclusion that while the introduction of dish slots causes a slight softening of the reflector, overall the effect on the deployed stiffness is nearly negligible.

If this line of reasoning is carried through then the extra set of rim slits on the DeSSRA design compared to the SSBR is the main contributor of the 3.8% decrease in deployed frequencies. This is backed up by an extra simulation of a design with the 8 rim slits of the DeSSRA model but without any dish slots (similar to the SSBR design). This hybrid design has a deployed frequency of 13.602 Hz and hence the extra rim slits result in a 3.7% decrease in frequency.

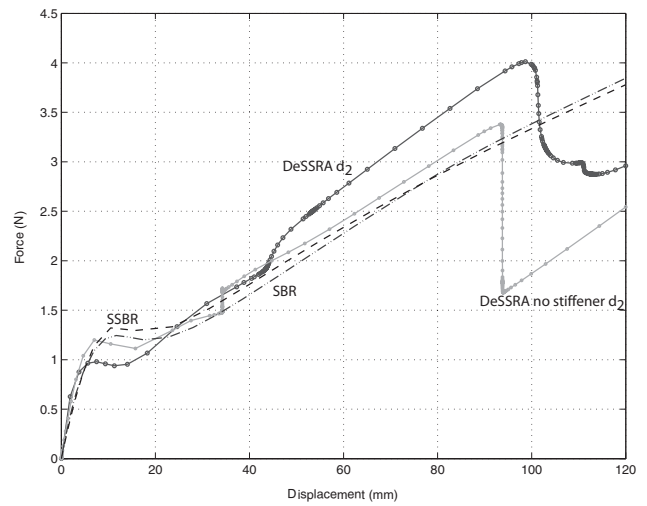
As to be expected, Table 1 and Figure 9 show that DeSSRA has the highest packaged stresses, the maximum stress for this general configuration currently exceeds the yield stress of the material however it is expected that a more optimal configuration will have lower stresses – increasing the slot lengths will lower these peak stresses. Figure 9 also shows that the location of the slots dictate the areas of the dish which experience folding and hence affect the stowage ratio.



(a) DeSSRA configurations



(b) Stiffened Configurations



(c) Diameter 2 response

FIG. 8: Comparison of force displacement behaviour of the packaging process

Config	DeSSRA		DeSSRA no stiffener		SSBR	SBR
	$d_1$	$d_2$	$d_1$	$d_2$		
$f$ (Hz)		13.6		5.8	14.1	5.9
$k$ (N/mm)	0.37	0.33	0.3	0.28	0.22	0.17
$\sigma_{max}$ (N/mm <sup>2</sup> )		80		54	75	50
$F_{snap}$ (N)	2.78	4.01	2.10	3.38	1.32	1.24
$F_{final}$ (N)	4.47	2.96	3.79	2.54	3.84	3.78
$m$ (grams)		263		231	271	235
$\eta$		2.8		2.7	4.4	4.1

TAB. 1: Comparison of different designs

In order to provide quantitative measure of the packaging efficiencies of the different designs, Greschik's [3] measure of the stowage ratio,  $\eta$  was adopted

$$(3) \quad \eta = \frac{\text{stowage envelope's surface area}}{\text{deployed aperture surface area}}$$

Table 1 lists the respective stowage ratio and shows that this non optimal DeSSRA configuration already has a stowage ratio which is 35% better than the SSBR.

The initial resistance to folding,  $k$  for DeSSRA is at least 50% higher than that of the SSBR, while the difference in the packaged stress is only 6% higher. Comparison with the unstiffened DeSSRA configuration shows that the stiffener accounts for about a 20% increase in initial stiffness.

The force-displacement behaviour of the packaging process of both the slotted shell designs is shown in Figure 8(a). The behaviour is very interesting, with marked differences depending on the loading diameter and is a result of the 4-way folding regime. The different force displacement characteristics along the second diameter are due to the staggered positioning of the dish slots. The correlation between the stiffened and unstiffened slotted shell designs along the respective diameters is very clear. There are two pronounced 'snaps' where the packaging forces reduce very suddenly. The first snap occurs at 34 mm displacement for the unstiffened case and 44 mm for DeSSRA, this corresponds to Quadrants I and III of the dish buckling towards the hub i.e. the curvature in the circumferential direction inverting. While the second snap occurs at displacements of 94 mm and 101 mm for the unstiffened and stiffened cases respectively and corresponds to the buckling of Quadrants II and IV. The second snap occurs much later due to the fact that these quadrants have a wider radius  $r_2 < r_1$  and are hence more resistant to buckling. The delayed snapping of the DeSSRA model compared to the unstiffened case is due to the stiffener which inhibits the movement of the dish.

Apart from causing a decrease in resistance along diameter  $d_1$  the sudden inversion of the curvature of diametrically opposite quadrants results in an abrupt increase of force in the perpendicular  $d_2$  direction, and vice versa. The magnitude of these snaps are listed in Table 2. The DeSSRA design is such that the force 'drops' are always larger than the corresponding force 'jumps' in the perpendicular direction. The ratio of the force jump to the force drop is the snap ratio,  $\Delta$  which is an indication of the magnitude of the force increase along one direction compared to the decrease in the other, hence lower snap ratios indicate large force drops and small corresponding force jumps.

	DeSSRA			DeSSRA no stiffener		
	$d_1$	$d_2$	$\Delta(\%)$	$d_1$	$d_2$	$\Delta(\%)$
1st snap	-1.26	0.58	46	-1.87	0.21	10
2nd snap	0.91	-1.05	82	0.73	-1.69	41

TAB. 2: Force jumps and drops (negative values) in Newtons. Snap ratio,  $\Delta = \frac{\text{force jump}}{\text{force drop}}$

From Figure 8 (a) the unstiffened configuration (DeSSRA no stiffener) has more abrupt snapping behaviours and also lower snap ratios, 10% and 41% compared to that of the DeSSRA model 46% and 82%. This is due to the fact that the presence of the stiffener in the DeSSRA configuration restricts the free movement of the rim of the dish, resulting in more gradual force transitions. Compared to the slotted shell design without a stiffener, DeSSRA reaches 31% and 18% higher snapping forces for diameters  $d_1$  and  $d_2$  respectively.

Next the packaging behaviour of DeSSRA compared to the SSBR is shown in Figure 8 (b). The initial stiffness along both diameters of DeSSRA is higher than the SSBR and the final packaged forces  $F_{final}$  are 16% higher and 22% lower than the SSBR along the  $d_1$  and  $d_2$  diameters respectively. Figure 8 (c) illustrates the force response along diameter  $d_2$  and demonstrates that apart from the snaps towards the end of the regime the behaviour is very similar to that of the 2-way folding of the configurations without dish slots i.e. SBR and SSBR.

The fact that both the stiffened and unstiffened DeSSRA designs are loaded at 4 points while the SSBR is only loaded at 2 points, also explains the higher initial stiffness of the unstiffened DeSSRA compared to the SSBR.

From the stress distribution plots (Figure 9) the highest stress concentrations occur at the edge of the loaded regions and hence with more careful design the peak packaged stresses can be reduced.

The packaging experiments shown in Fig. 10, show excellent agreement in the initial stiffness regime, while the finite element simulations and experimental results show similar trends for the large displacement regime. However the physical model tends to buckle earlier about both diameters  $d_1$  and  $d_2$  and reach higher second force peaks. This is mainly due to inaccuracies of cutting out the slots which affect the magnitude and timing of quadrant inversion and also the symmetry of the model. It is worth noting that the physical models used for the experiments have a wider stiffener and a smaller diameter due to limitations

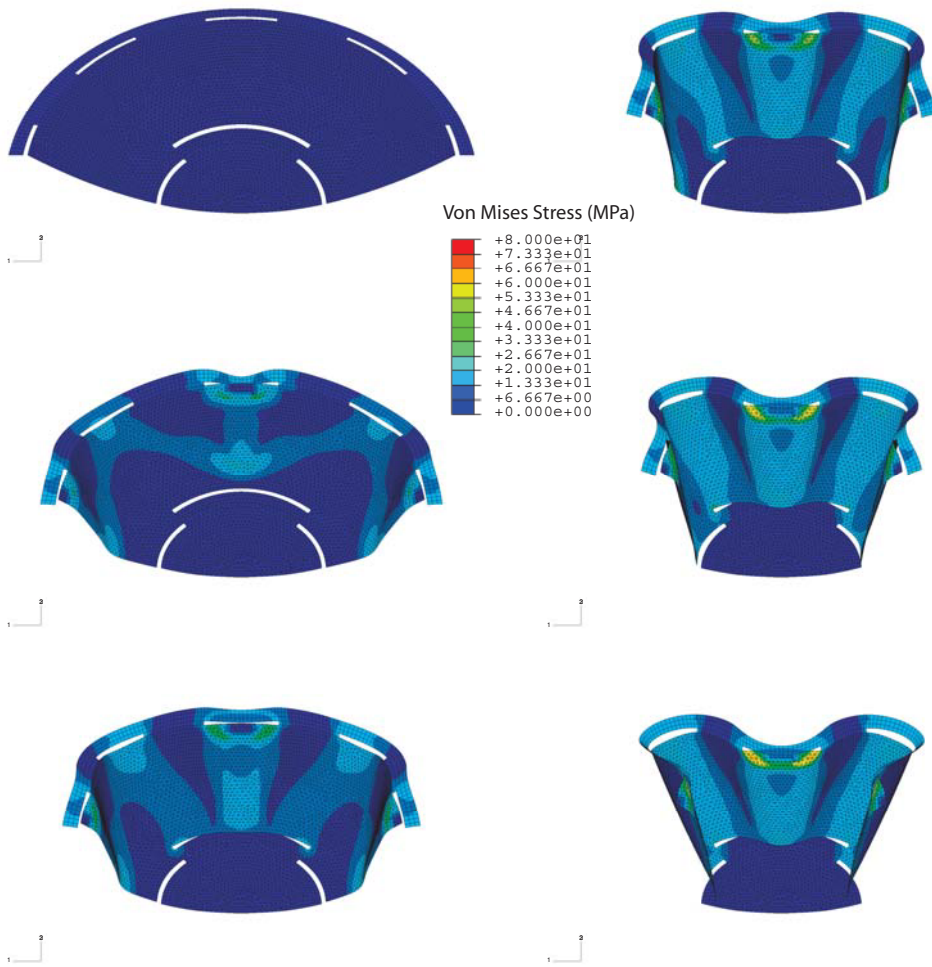


FIG. 9: Folding sequence of reflector

in the manufacturing machinery, and hence the packaging behaviour in Figs 8 and 10 are of course different. The more pronounced first buckling peak in Fig. 10 is due to the wider stiffener.

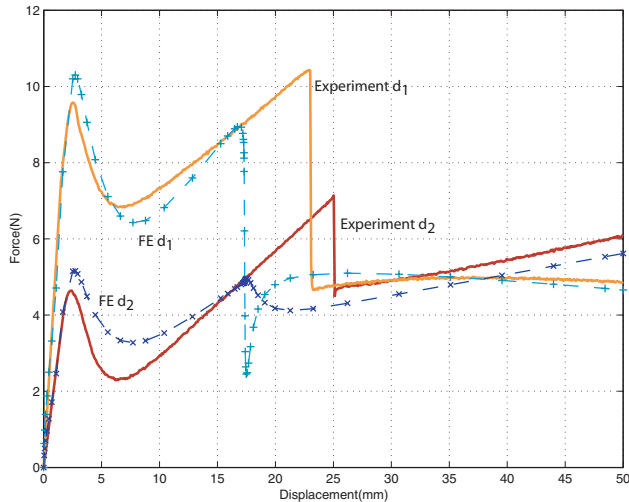


FIG. 10: Packaging behaviour experimental and finite element results

## 7. CONCLUSIONS

A petalized design with radial cuts and a much better stowage efficiency was also considered, but although the stiffening rim helps to maintain the overall deployed shape, the deployed fundamental frequency is nearly halved and the problem of reconnecting the petal edges together after deployment still persists. Hence circumferential rather than radial continuity in slotted shell reflectors is the more crucial for both shape accuracy and overall structural stiffness.

Compared to the SSBR design (the current highest stiffness single-piece thin shell deployable reflector), the experimentally verified DeSSRA design achieves a 35% increase in stowage efficiency with a more uniform aspect ratio, a 50% increase in the initial resistance to folding while the continuous rim stiffener maintains a high deployed stiffness (only 3.5% less than the SSBR), and hence good shape accuracy. These values are expected to improve further with optimization of the design parameters.

## 8. ACKNOWLEDGEMENTS

Thanks go to S.Norager for the preliminary designs and finite element analyses and S.Harland for some of the experimental work.

## REFERENCES

- [1] BLEVINS, R. D. *Formulas for Natural Frequency and Mode Shapes*. Krieger Publishing Company, ch. 12, pp. 330–334.
- [2] DATASHVILI, L., LANG, M., ZAUNER, C., BAIER, H., SOYKASAP, O., TAN, L. T., KUEH, A., AND PELLEGRINO, S. Technical assesment of high accuracy large

space borne reflector antenna (tahara). Technical Report ESA Contract number 16757/02/NL/LvH/bj, Technical University of Munich, 2005. Ref.: LLB-R-12/07/04-02D-02.

- [3] GRESCHIK, G. On the practicality of a family of pop-up reflectors. In *9th Annual AIAA/Utah State University Conference on Small Satellites* (18-21 September 1995).
- [4] HIBBITT, KARLSSON, AND SORENSON. *ABAQUS Standard Users Manual Version 6.1*. Hibbitt, Karlsson and Sorenson, Hibbitt, Karlsson & Sorenson, 1080 Main Street Pawtucket, Rhode Island 02860-4847, USA, 1998.
- [5] ROBINSON, S. A. Simplified spacecraft antenna reflector for stowage in confined envelopes. Publication number: 0534110A1, 31 March 1993. European Patent Application filed by Hughes Aircraft Company.
- [6] ROGERS, C. A., AND STUTZMANN, W. L. Large deployable antenna program, phase 1: Technology assessment and mission architecture. Contractor Report NAS1-18471, NASA, October 1991.
- [7] ROMEO, R. C., MEINEL, A. B., MEINEL, M. P., AND CHEN, P. C. Ultra-lightweight and hyper-thin rollable primary mirror for space telescopes. In *UV, Optical and IR Space Telescopes and Instruments, Proceedings of SPIE* (2000), J. Breckinridge, Ed., vol. 4013, pp. 634–639.
- [8] TAN, L. T. *Thin-Walled Elastically Foldable Reflector Structures*. PhD thesis, Department of Engineering, University of Cambridge, Cambridge, CB2 1PZ, UK, December 2002.
- [9] TAN, L. T., AND PELLEGRINO, S. Stiffened spring back reflectors. In *25th ESA Antenna Workshop on Satellite Antenna Technology*, (ESTEC, Noordwijk, The Netherlands, 18-20 September 2002), pp. 755–762.
- [10] TAN, L. T., AND PELLEGRINO, S. Stiffness design for spring back reflectors. In *43rd AIAA/ASME/ASCE/AHS/ASC Structures, Structural Dynamics and Materials Conference* (Denver Colorado, 22-25 April 2002). AIAA 2002-1498.
- [11] TAN, L. T., AND PELLEGRINO, S. Stiffening method for thin shell deployable reflectors: Part 1, approach. *AIAA Journal* 44, 11 (November 2006), 2515–2523.
- [12] TAN, L. T., SOYKASAP, O., AND PELLEGRINO, S. Design & manufacture of stiffened spring-back reflector demonstrator. In *46th AIAA/ASME/ASCE/AHS/ASC Structures, Structural Dynamics and Materials Conference* (Austin, Texas, April 2005).
- [13] TIBBALDS, B., GUEST, S. D., AND PELLEGRINO, S. Inextensional packaging of thin shell slit reflectors. *Technische Mechanik* 24, 3-4 (2004), 211–220.